INTERNATIONAL JOURNAL OF INTEGRATED ENGINEERING
ISSN: 2229-838X e-ISSN: 2600-7916

IJIE

Vol. 16 No. 5 (2024) 162-171
https://publisher.uthm.edu.my/ojs/index.php/ijie

A Study of Automatic Pineapple Leaf Fibre Extraction Machine Using Bidirectional Rolling Mechanism

Van-Tinh Nguyen[1]*, Ngoc-Kien Nguyen[1]

[1] *School of Mechanical Engineering,*
Hanoi University of Science and Technology, Hanoi, VIETNAM

*Corresponding Author: tinh.nguyenvan@hust.edu.vn
DOI: https://doi.org/10.30880/ijie.2024.16.05.013

Article Info

Received: 25 November 2023
Accepted: 29 May 2024
Available online: 1 August 2024

Keywords

Pineapple leaf fibre, extraction, machine, design, LS-DYNA

Abstract

Pineapple leaf fibres are well known around the world due to the good material properties when woven together and environment friendly. Nevertheless, it takes a lot of effort and time to extract the fibres from the pineapple leaves. Consequently, various machines have been constructed around the world to automate this process, which has helped save time and increased the output productivity remarkably. This paper proposed a novel design of the automatic pineapple leaf fibre extraction machine using bidirectional rolling mechanism. The proposed mechanism will improve the efficiency of the pineapple leaf fibre extraction process that simultaneously enhances the quality of the output fibres.

1. Introduction

For thousands of years, agriculture has played an important role in everyday life. Agriculture plays a crucial role in decreasing poverty, increasing incomes, and enhancing food security for the majority of the world's poor, who reside in rural areas and mainly engaged in farming activities. Additionally, agriculture is also essential to economic growth, it contributes 4% to the global gross domestic product (GDP), especially it can be more than 25% of GDP in some least developing countries [1]. Therefore, humans continuously developed tools and practices to improve agricultural output.

The history of agriculture's automation witnesses various automatic machines and systems conceptualized, fabricated, and developed. For instance, ZhaoDe-An et. al. and colleagues introduced an autonomous robot for harvesting apples, incorporating a manipulator, end-effectors, and image-based servo systems in its system [2]. Likewise, X. Ni et. al. introduced a design for an apple-picking robot that utilizes image recognition techniques [3]. W Lili et. al. conducted research to create a tomato harvesting robot, employing a laser navigation control system in conjunction with the proportional-integral-derivative (PID) algorithm [4]. Li, Shichao et. al. constructed an autonomous navigation system for agricultural machinery which comprises a master and a slave agricultural machinery, the slave follows the master to perform an automatic navigation task [5]. In addition, several researchers have contributed publications on designing automatic machines including plucking machines [6-10] and machines designed for automatic fruit harvesting [11-13].

Pineapple is a type of bromeliad plant that lives for many years. These leaves are enveloped by an epidermal layer, containing the essential parenchyma tissue with delicate-walled cells. Within this tissue, there are diverse bundles of fibers with varying diameters [14]. Observation on characteristics of pineapple fibers, the tensile strength and resilience are remarkable points. Besides, their abundant presence in nature contributes to the development of sustainable and environmentally friendly production methods. One of popular products from pineapple fibres is silk which is fabricated by weaving the fibres together. Pineapple silk possesses durability, strength, and properties comparable to traditional ones. In the conventional method, the extraction process of

pineapple fiber is implemented by manual which consists of three stages such as preparation of pineapple leaves, scratching of leaves, and extraction of fibers [15].

During the leaf preparation stage, the surface of the leaf undergoes a thorough cleaning to remove any dust or soil, simultaneously the withered or rotten leaves are eliminated. In addition, this stage is to cut off the thorns on two rears of the leaves. In the next stage, the flesh of the leaf is delicately scratched to reveal the fibers. The final step involves extracting the fibers from the scratched pineapple leaves, followed by a thorough washing and drying process. Afterwards, the fibers undergo chemical treatment to prepare for the weaving process. As can be concluded that the conventional method is time-consuming and low efficiency, with no guarantee of the extracted fibers' quality. To improve the efficiency of the pineapple leaf fibre extraction process in the future, it is crucial to automate the entire process.

The field of fibre extraction observed numerous automatic machines which were studied to replace the traditional technique. To be illustration, C. Veera ajay et. al. presented a manually operated machine designed for extracting banana fibers [16]. Likewise, an automatic extraction machine was developed by Sachin Poudel and his colleagues [17]. In addition, a jute fibre extraction machine was designed and evaluated by Md. Rejaul Karim et. al. [18]. Especially, James McCrae invented a leaf fibre extraction apparatus [19] while Zhangjiagang Shengtai fibre company created an extraction device for fibre in plant stems and leaves [20]. Moreover, Nguyen, NK. and Nguyen, VT introduced the first prototype of lotus fiber extracting machine [21]. However, the disadvantage of the previous studies is that the input leaves move gradually in one-way direction, leading to a difficulty in obtaining perfectly clean output fibers.

This paper introduced a novel prototype of the pineapple leaf fibres extracting machine using bidirectional rolling mechanism. It is implemented by a planetary cam-gear system which creates the bidirectional motion of the input material and makes the output fibre cleaner. The efficiency of the new machine was confirmed through the simulation and experiment results. The remains of this paper are organized into three sections such as Section 2 addressed to the principle and structure of the proposed machine, Section 3 presented the simulation model and experiment, finally, Section 4 included some conclusions.

2. Design of Proposed Machine Structures

2.1 Working Principle

The principal diagram of the proposed machine is described in Figure 1. After harvesting process, the pineapple leaves undergo a cleaning procedure to remove dust and soil, simultaneously eliminating any low-quality leaves. The processed leaves are fed and rolled by two rollers; the rollers have a role in clamping the leaves while it is scratched by the blades of the rolling cage. In this process, the rollers employed a bidirectional rotation mechanism to repetitively scratch the leaves. Consequently, the blades will remove the epidermis and retain the fibres, the pineapple leaf fibres will be stripped of its parenchymal tissue and taken to the conveyor to bring outside. To easily assemble and maintain, the machine is separated into four modules such as rollers, scratching cage, conveyor, and frame.

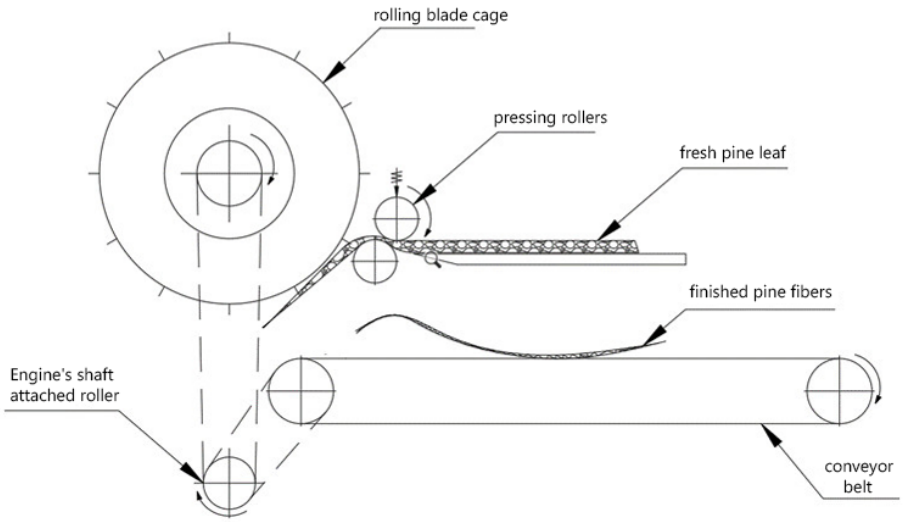

Fig. 1 *Principal diagram of the proposed machine*

Int. Journal of Integrated Engineering Vol. 16 No. 5 (2024) p. 162-171

2.2 Transmission System of Power

The motion of three components such as rollers, cage, and conveyor are actuated by a DC motor only. Torques from the motor's shaft is transmitted via reducer box and belt systems. The rollers have dual role in clamping and guiding the leaf into the scratching cage while the blades were used to scratch and remove the leaf's flesh. After this stage, the fibre will be exposed and collected on the below conveyor. In addition, to ensure safety of the system, when the motor's overload occurs, the belts will slip and separate the movement between the driving and driven shaft.

Through experiment, the leaves need feeding into the machine at a rate of 1000 mm/min. To do this, the rollers require to rotate at 20 rpm. Simultaneously, the conveyor-driven rollers maintain a speed of 60 rpm, and the rolling blade cage operates at 800 rpm. Figure 2 shows a structural diagram of the proposed machine in which GT refers to the reducer box; I corresponds to the shaft of the rolling blade cage; II represents the intermediary shaft; III denotes the shaft of the driving pulley, IV stands for the driving shaft of the gear transmission, finally, V designates for the driven shaft of the gear transmission.

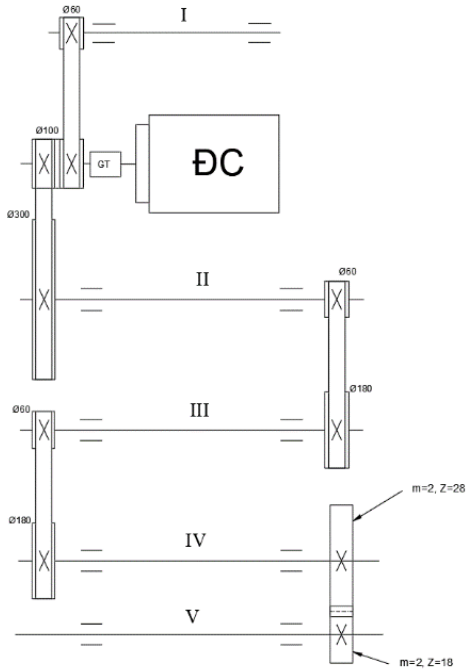

Fig. 2 *Power transmission diagram*

The power of DC motor is expressed as Equation 1.

$$P_{dc} = \left(\frac{P_l}{\eta_l} + \frac{P_e}{\eta_e} + \frac{P_b}{\eta_b} + \frac{P_r}{\eta_r}\right) * s \tag{1}$$

Where P_{dc}, P_l, P_e, P_b, and P_r are shaft power of motor, cage, roller, conveyor, and pinion gear, respectively, η_l, η_e, η_b, and η_r are coefficient of efficiency on the shaft of cage, roller, conveyor, and pinion gear, respectively, $\eta_l = 0.93$; $\eta_e = 0{,}84$; $\eta_b = 0.88$; $\eta_r = 0.85$; s is overload factor, s is selected to 2.

The shaft power of cage is expressed as Equation 2.

$$P_l = (I + M_l) * \omega_l = \left(\frac{1}{2} m * {r_l}^2 + F * r_l\right) * 2\pi * n_l$$
$$= \left(\frac{1}{2} * 10 * 0.15^2 + 50 * 0.15\right) * 2\pi * \frac{833}{60} = 664.05\ (W) \tag{2}$$

Where I is inertial moment, ω_l is angular velocity of the cage, M_l is torque from the blades, r_l is a radius of the cage, F is a force from the blade acting on the pineapple leaf.

The shaft power of rollers is expressed as Equation 3.

$$P_e = M_e * \omega_e = F_e * r_e * 2\pi * n_e = 300 * \frac{0.06}{2} * 2\pi * \frac{20}{60} = 18.85\ (W) \tag{3}$$

Where F_e is friction force between the roller and the leaf, r_e is a radius of the roller, n_e is velocity of the roller, ω_e is an angular velocity of the roller.

The shaft power of conveyor is expressed as Equation 4.

$$P_b = M_b * \omega_b = Q_b * \mu * r_b * 2\pi * n_b = 100 * 0.25 * \frac{0,06}{2} * 2\pi * \frac{60}{60} = 4.71\ (W) \quad (4)$$

Where Q_b is the load in the working process, μ is a friction factor, r_b is a radius of the conveyor's roller, ω_b is an angular velocity of the roller, n_b is velocity of the conveyor's roller.

The shaft power of pinion gear is expressed as Equation 5.

$$P_r = M_r * \omega_r = F_r * r_r * 2\pi * n_r = \frac{2.833}{2.28} * \frac{2.28*10^{-3}}{2} * 2\pi * \frac{12}{60} = 1.8\ (W) \quad (5)$$

Where F_r is tangential force on pinion gear, r_r is a reference radius of the pinion gear, ω_r is an angular velocity of the pinion gear, n_r is a velocity of the pinion gear.

Finally, the power of DC motor is calculated by Equation 6.

$$P_{dc} = \left(\frac{P_l}{\eta_l} + \frac{P_e}{\eta_e} + \frac{P_b}{\eta_b} + \frac{P_r}{\eta_r}\right) * s = \left(\frac{664.05}{0.93} + \frac{18.85}{0.84} + \frac{4.71}{0.88} + \frac{1.8}{0.85}\right) * 2 = 1487.89\ (W) \quad (6)$$

The output power of DC motor is selected to 1500W and a spindle's rotation speed of 1500 rpm, the gear reducer box has the transmission ratio of $u_{hgt} = 1:3$ resulting in a driven shaft speed of $n_1 = n_{dc}/u_{hgt} = 1500/3 = 500$ rpm, where n_{dc} is the motor's spindle speed.

The blade cage's speed is calculated by Equation 7.

$$n_l = n_1 . u_1 = 500 . \frac{5}{3} = 833\ (rpm) \quad (7)$$

Where u_1 is a speed ratio of belt transmission mechanism, $u_1 = 5/3$.

2.3 Design of Scratch Cage

Figure 3 displays the 3D model of the scratching cage which was created using SolidWorks tools (CAD software, Dassault System). The material of the cage is a heat-treated steel C45 which has a yield stress of 330-460 MPa, tensile strength of 570-700 MPa.

To avoid the slip phenomenon, the tensile force of the belt needs to satisfy Equation 8.

$$F_0 \geq \frac{F_t}{2} * \frac{e^{f'*\alpha}+1}{e^{f'*\alpha}-1} \quad (8)$$

Where F_o is tensile force, F_t is tangential force on pulley, f' is converted friction factor, α is an angle of belt contact.

Where the tangential force on pulley is expressed by Equation 9.

$$F_t = \frac{1000P}{v_2} = \frac{1000P}{\frac{\pi*d_2*n_2}{60000}} = \frac{6*10^7*0.67}{\pi*63*1500*\frac{63}{100}} = 214.93\ (N) \quad (9)$$

With P is motor power, d_2 is driving pully diameter, n_2 is velocity of pulley. The converted friction factor is determined by Equation 10.

$$f' = \frac{f}{sin\left(\frac{\theta}{2}\right)} = \frac{0,2}{sin\left(\frac{40^\circ}{2}\right)} = 0.585 \quad (10)$$

With f is friction factor between pulley and belt, θ is wedge angle of belt. The angle of belt contact is described by Equation 11.

$$\alpha_1 = 180 - (d_2 - d_1) * \frac{57}{a} = 180 - 37 * \frac{57}{430} = 174.98^\circ = 3.05\ (rad) \quad (11)$$

With d_1 is driven pulley diameter, a is distance of pulley centers. Finally, the minimum tensile force of the belt is calculated by Equation 12.

$$F_0 \geq \frac{F_t}{2} * \frac{e^{f'*\alpha}+1}{e^{f'*\alpha}-1} = \frac{214.93}{2} * \frac{e^{0.585*3.05}+1}{e^{0.585*3.05}-1} = 314.17\ (N) \quad (12)$$

Int. Journal of Integrated Engineering Vol. 16 No. 5 (2024) p. 162-171

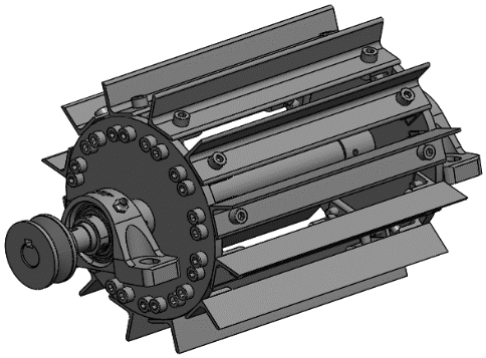

Fig. 3 *Scratching cage*

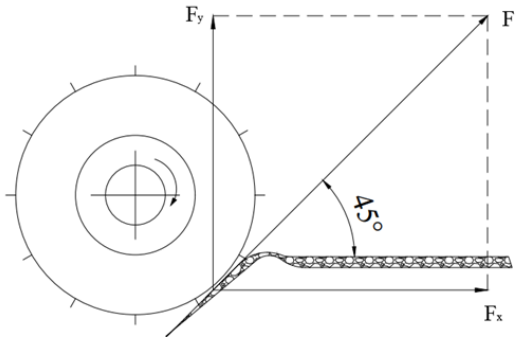

Fig. 4 *Force applied onto the leaf by the blade*

Figure 4, the principle of the pineapple fibre extracting process is illustrated. As can be seen, the leaf gradually enters the working area, at the same time the blade will rotate and scratch on the leaf to progressively eliminate the flesh. The fibre is guided to the below conveyor belt to carry outside.

The shaft diameter of the cage is expressed by Equation 13.

$$d_j = \sqrt[3]{\frac{M_{tdj}}{0.1[\sigma]}} \tag{13}$$

Where d_j is diameter of shaft division, $[\sigma]$ is yield point of material, $[\sigma]$=600 Mpa, M_{tdj} is converted inertial moment presented by Equation 14.

$$M_{td} = \sqrt{{M_j}^2 + 0{,}75 * {T_j}^2} \tag{14}$$

Where T is torque, M_j is the total bending moment and is determined by Equation 15.

$$M_j = \sqrt{{M_{xj}}^2 + {M_{yj}}^2} \tag{15}$$

Diagram of the force acting on the cage's shaft as presented in Figure 5. Contact angle between the blade and pineapple leaf, $\alpha = 45^o$, force to remove the layer of epidermis is defined by experiment, F=*50N*, the length of shaft segments $l_1 = 46\ mm, l_2 = 242\ mm,\ l_3 = 334\ mm, l_4 = 67\ mm$.

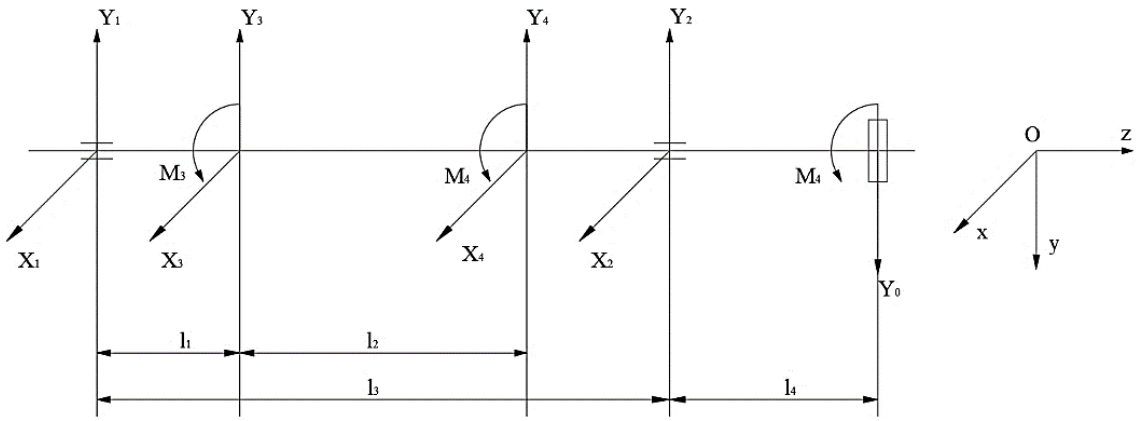

Fig. 5 *Diagram of the force acting on the cage's shaft*

Set of equations are expressed in Equation 16-19.

$$\sum F_{xt} = X_1 + X_2 + X_3 + X_4 = 0 \tag{16}$$

$$\sum F_{yt} = -Y_0 + Y_1 + Y_2 + Y_3 + Y_4 = 0 \quad (17)$$

$$\sum M_x(0) = X_3 * l_1 + X_4 * (l_1 + l_2) + X_2 * l_3 = 0 \quad (18)$$

$$\sum M_y(0) = Y_3 * l_1 + Y_4 * (l_1 + l_2) + Y_2 * l_3 - Y_0 * (l_3 + l_4) = 0 \quad (19)$$

With $X_3 = X_4 = Y_3 = Y_4 = \frac{F*sin(\alpha)}{2} = \frac{50*sin(45^o)}{2} = 35.36\ (N)$.

After solving Equation 16-19, the obtained solutions are as follows: $X_1 = -17.68$ N; $X_2 = -17.68$ N; $Y_1 = -80.7$ N; $Y_2 = 359.51$ N. Moreover, the results of moments are calculated as M_{td1} = 3813.87 Nmm; M_{td2} = 18992.64 Nmm; M_{td3} = 21059.09 Nmm; M_{td4} = 639.13 Nmm. Substituting the converted inertial moment to Equation 13, the estimated diameters for the shaft segments are found to be: d_o = 5.22 mm; d_1 = 8.46 mm; d_2 = 14.45 mm; d_3 = 14.95 mm. However, for practical fabrication considerations, the structure of the shaft is selected as follows: d_o = 16 mm; d_1 = 20 mm; d_2 = 18 mm; d_3 = 15 mm.

2.4 Design of Bidirectional Rolling Mechanism

In Figure 6, rollers (1) and (2) play a crucial role in ensuring grip of the leaves, leading to allowing the blade to have sufficient time to thoroughly clean the leaf's flesh. Through the experiments, these rollers need to operate at a speed of 20 rpm while the leaf moves at a speed of 0.06 m/s. Consequently, a diameter of 60mm is selected for the rollers. On the right side of Figure 6 is zoom out of a planetary cam-gear mechanism which consists of a spur gear and an internal and external cam-gear, is designed to create bidirectional rolling motion of the rollers. Firstly, the leaves will be supplied to rollers for beginning of scratch. After a certain interval, the leaves are retracted for a secondary scratch. These cyclic processes continue until the leaves exit the rollers. The principal diagram of this mechanism is shown in Figure 7.

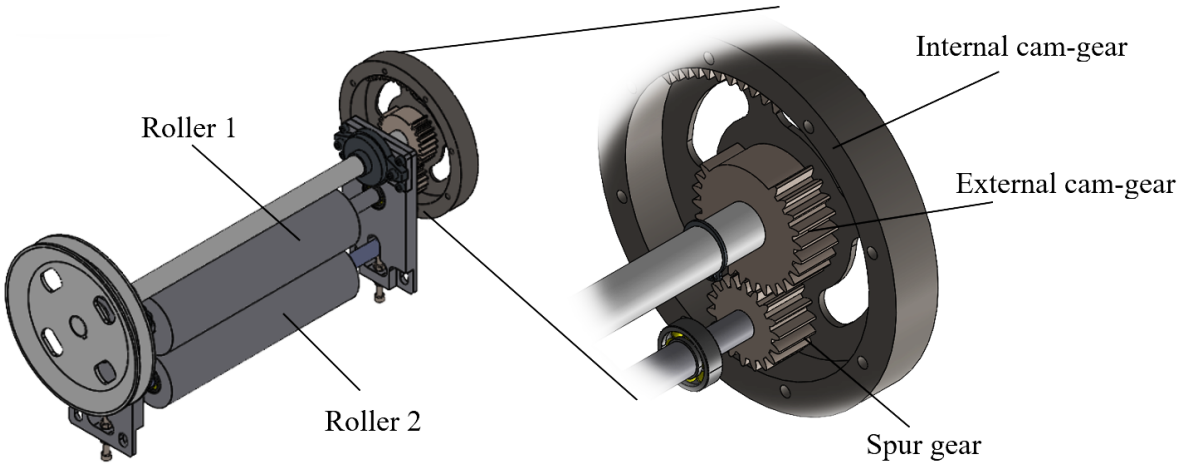

Fig. 6 *3D model of roller with planetary cam-gear mechanism*

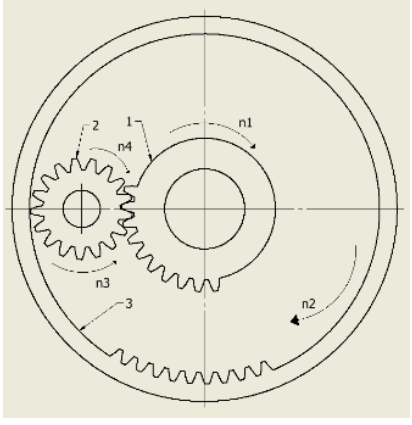

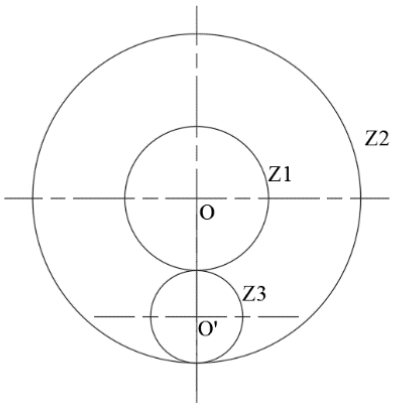

Int. Journal of Integrated Engineering Vol. 16 No. 5 (2024) p. 162-171

Fig. 7 *Planetary cam-gear mechanism*

Assuming that Z_1 is the number of sun gear, Z_2 is the number of internal gears and Z_3 is the number of planet gear, geometric condition of the planetary gear system as expressed by Equation 20.

$$Z_2 = Z_1 + 2 * Z_3 \tag{20}$$

Dividing Equation 20 to Z_3, obtaining Equation 21.

$$\frac{Z_2}{Z_3} = \frac{Z_1}{Z_3} + 2 \tag{21}$$

Set $T_1 = \frac{Z_1}{Z_3}$; $T_2 = \frac{Z_2}{Z_3}$, leading to $T_2 = T_1 + 2$

If the percentage of remaining tooth number of the sun gear is a %, the percentage of remaining tooth number of the sun gear is (1- a) %. The ratio of the length of journey in forward and backward direction is presented by Equation 22.

$$\frac{S_d}{S_v} = b = \frac{a*T_1}{(1-a)*(T_1+2)} \tag{22}$$

Due to constraint conditions of working space, this research selected $Z_3 = 18$; $Z_1 = 28$, thus $Z_2 = 64$. Assuming that the length of journey in forward direction is double times in the backward one, b=2. Solving Equation 22 obtained a=0.82, thus, the remaining tooth number of the sun and internal gear, $Z_1' = 0.8205 * 28 = 22.974$ (23 teeth); $Z_2' = (1 - 0.8205) * 64 = 11.487$ (11 teeth).

In summary, the comprehensive 3D model of the proposed machine is designed using SolidWorks 2020 as depicted in Figure 8. The machine comprises four main components such as rollers with planetary cam-gear mechanism, scratching cage, conveyor belt, and a frame. The entire motion of the proposed machine is actuated by a DC motor only.

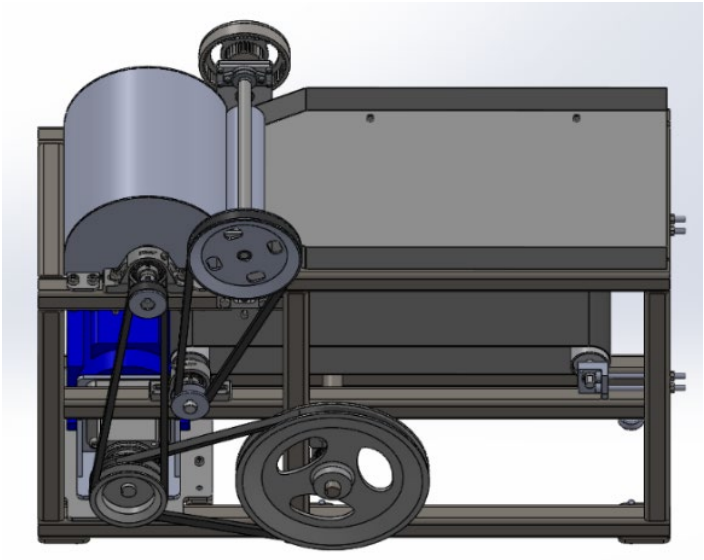

Fig. 8 *3D model of entire proposed machine*

3. Results and Discussion

3.1 Simulation of Fibre Extraction Process

Before fabrication, simulation is needed to verify the design of the machine that will save time and significantly diminish the overall cost of fabricating the machine [22-24]. To investigate the deformation of the leaf and the generation of pineapple leaf fibers, this study simulated the interaction between a leaf and the roller system as

well as scratching cage. The simulation file was set up using LS-PrePost and executed in LS-DYNA (CAE software, Livermore Software Technology Corporation).

In order to focus solely on understanding of the pineapple leaf's reactions during machine operation, the 3D model of the machine was simplified by only retaining the rollers and the scratching cage that also helps reduce computational cost and time saving. As a result, the simulation model remains as shown in Figure 9. The next step involved importing it into LS-DYNA for obtaining the meshed model as presented in Figure 10.

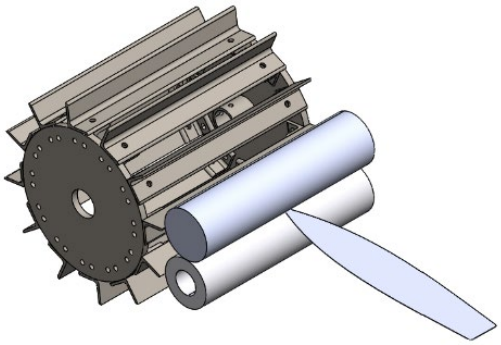

Fig. 9 *Simulation model in SolidWorks*

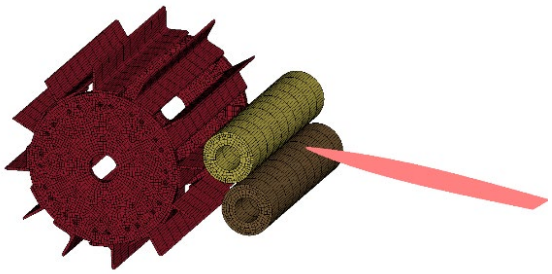

Fig. 10 *Meshing process in LS-DYNA*

The scratching cage and rollers were meshed by the solid meshing method and are divided into 28361 elements while the pineapple leaf adopted Smoothed Particle Hydrodynamics (SPH) model, it is divided into 83952 particles. The reason is that SPH model is most suitable for highly deformable models by representing them with discrete particles. This method was usually selected for complicated simulation processes because of its ability to obtain accurate results while saving computational time. The AUTOMATIC_NODES_TO_SURFACE card with node set type 4 was used as a contact between leaf and blade, roller. To set the movement of the leaf, roller and blade, CURVE card is used.

The blade and the rollers are made of C45 steel, the properties of this material are detailed as follows: density of 7850 (kg/cm3), Young's modulus of 205000 MPa, and Poisson's number of 0.3 [25]. For simulation, it was supposed to be completely rigid and was modeled by MAT_RIGID card. On the other hand, the properties of the pineapple leaves are density of 1.526 (g/cm3), tensile strength of 170 MPa, and Young's modulus of 6260 [26]. The simulation duration is configured for 3 seconds that ensures sufficient time for deformation and fiber extraction while reducing processing time.

The output data is presented in a D3PLOT file, the sampling period in the NODOUT data was set to 0.1 seconds to decrease the collected points and prevent the results from aliasing phenomena. The executive time was approximately 4 hours when running on Lab's computer with the configuration of 64G RAM, Ryzen 9 3900X (3.8 GHz, 70MB cache 12C/24T) chip.

The simulation results depicted in Figure 11 reveal that under the pressure of the rollers, the leaf moves gradually heading to the blades as presented in Figure 11a. The leaf's flesh is extracted into numerous particles and drops down as shown in Figure 11b.

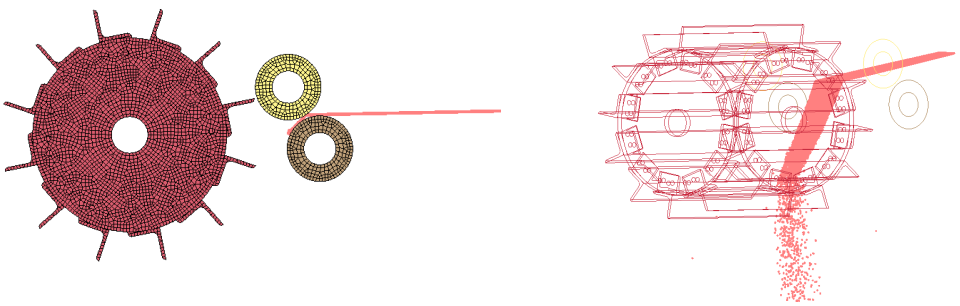

(a) **(b)**

Fig. 11 *Simulation result (a) Feeding process; (b) Pineapple fibre extraction*

Int. Journal of Integrated Engineering Vol. 16 No. 5 (2024) p. 162-171

3.2 Fabrication of The Proposed Machine

Figure 12a presents the fabrication of the proposed automatic pineapple leaf fibre extraction machine. The specifications are described as follows: 980mm length, 750mm width, 535mm height, and weight of 90.5 kg. To reach the best performance, the pineapple leaves are required within specific dimensions such as a length within the range of 200 to 300 mm while a width between 10 to 15 mm. The machine achieves a productivity rate of 10-15 leaves per minute corresponding to 4-5 kilogram per hour that is 1.5 times more efficient than the handcrafted method. In addition to significantly enhancing yield, the proposed machine guarantees the quality of the extracted fibers as depicted in Figure 12b. The planetary cam-gear mechanism works properly to create the bidirectional motion, that makes the fibre cleaner. To consider the performance of the new machine, 30 test runs were conducted. As a result, the success rate of fibre extraction is 27, accounting for 90%. A situation where the leaf was broken, and the leaf moved inside the scratching cage in two remaining situations.

Fig. 12 *Pineapple fibre extraction machine (a) Fabrication of machine; (b) Extracted pineapple fibre*

4. Conclusions

This research presented an innovative design of the automatic pineapple leaf fibre extraction machine which applied a bidirectional rolling mechanism to create the bidirectional motion of the input leaf and simulated the traditional pineapple leaf fibre extraction motion of the craftsman. The machine's 3D model is made using SolidWorks 2020, and the simulation of the fiber extraction process is implemented in LS-DYNA to analyze leaf behavior and determine the optimal structure for the proposed machine. Experimental results demonstrate that the machine smoothly operates with a high confidence level of 90%. By applying planetary cam-gear mechanism, the leaf will be scratched more times than the conventional fibre extraction machine. Remarkably, its productivity surpasses the traditional extraction process by 1.5 times while guaranteeing the quality in the produced fibers.

Acknowledgement

This research was partially supported by the Asahi Glass Foundation: AGF.2024-03.

Conflict of Interest

Authors declare that there is no conflict of interests regarding the publication of the paper.

Author Contribution

The authors confirm contribution to the paper as follows: ***study conception and design:*** *Van-Tinh Nguyen, Ngoc-Kien Nguyen;* ***data collection:*** *Ngoc-Kien Nguyen;* ***analysis and interpretation of results:*** *Van-Tinh Nguyen;* ***draft manuscript preparation:*** *Van-Tinh Nguyen;* ***revision:*** *Ngoc-Kien Nguyen. All authors reviewed the results and approved the final version of the manuscript.*

References

[1] Agriculture and Food. https://www.worldbank.org/en/topic/agriculture/overview
[2] Zhao De-An, Lv Jidong, Ji Wei, Zhang Ying, Chen Yu (2011) Design and control of an apple harvesting robot. Biosystems Engineering, Vol. 110, Is. 2, pp. 112-122.

[3] Xindong Ni, XinWang, ShumaoWang, ShuboWang, ZeYao, YiboMa (2018) Structure Design and Image Recognition Research of a Picking Device on the Apple Picking Robot. IFAC-PapersOnLine, Vol. 51, Is. 17, pp. 489-494.
[4] Wang Lili, Zhao Bo, Fan Jinwei, Hu Xiaoan, Wei Shu, Li Yashuo, Zhou Qiangbing, Wei Chongfeng (2017) Development of a tomato harvesting robot used in greenhouse. Int J Agric & Biol Eng., 10(4), pp. 140–149.
[5] Li, Shichao; Xu, Hongzhen; Ji, Yuhan; Cao, Ruyue; Zhang, Man; Li, Han (2019). Development of a following agricultural machinery automatic navigation system. Computers and Electronics in Agriculture, 158, 335–344
[6] Erada, J.C (2008) Traveling Type Tea Plucking Machine. JP Patent No. 2008301831.
[7] Aokiha, J.A (2011) Tea Leaf-Picking Mchine. JP Patent No. 2011193754.
[8] Hu, X.G. Dc (2012) Tea Plucking Machine. CN Patent No. 102668812 A.
[9] Long, C.H. (2012) A Kind of Tea Plucking Machine. CN Patent No. 202444808 U.
[10] Xiao, Y.H. (2012) A Kind of Tea Plucking Machine. CN Patent No. 202496217 U.
[11] Yoshida, T., Onishi, Y., Kawahara, T. et al. (2022) Automated harvesting by a dual-arm fruit harvesting robot. Robomech J 9, 19.
[12] Onishi, Y., Yoshida, T., Kurita, H. et al. (2019) An automated fruit harvesting robot by using deep learning. Robomech J 6, 13.
[13] Font, Davinia; Pallejà, Tomàs; Tresanchez, Marcel; Runcan, David; Moreno, Javier; Martínez, Dani; Teixidó, Mercè; Palacín, Jordi (2014). A Proposal for Automatic Fruit Harvesting by Combining a Low-Cost Stereovision Camera and a Robotic Arm. Sensors, 14(7), 11557–11579.
[14] Moya, R., Berrocal, A., Rodríguez-Zúñiga, A., Rodriguez-Solis, M., Villalobos-Barquero, V., Starbird, R., and Vega-Baudrit, J. (2016). Biopulp from pineapple leaf fibre produced by colonization with two white-rot fungi: Trametes versicolor and Pleurotus ostreatus, BioRes. 11(4), 8756-8776.
[15] Bassey Okon Samuel, Malachy Sumaila & Bashar Dan-asabe (2022) Cellulosic fibre reinforced hybrid composite (PxGyEz) optimization for low water absorption using the robust taguchi optimization technique, Jurnal Mekanikal, 45(2), pp. 1-20
[16] C. Veera ajay, K. Vignesh Ramamoorthy, V. Subash, R. Robinston, M. Ragashwar, C.T. Justus Panicker (2021). Design and fabrication of manually operated banana fibre extracting Machine for agriculture applications. In: Materials Today: Proceedings, Vol. 45, Part 9, pp. 8199-8202.
[17] Sachin Poudel, Sushil Chapai, Raj Kumar Subedi, Tark Raj Giri, Sunil Adhikari (2019). Design, fabrication and testing of banana fibre extraction machine, Journal of Innovation in Engineering Education, Vol. 2, Iss. 1, pp. 165-173
[18] Md. Rejaul Karim, Muhammad Arshadul Hoque, Alamgir Chawdhury, Faruk-Ul-Islam, Sharif Ahmed, Ayman EL Sabagh and Akbar Hossain (2021). Design, Development, and Performance Evaluation of a Power-Operated Jute Fibre Extraction Machine. AgriEngineering, 3(2), 403-422.
[19] James, Mccrae (US2722039) (1955). Apparatus for obtaining fibres from plant leaves.
[20] Zhangjiagang Shengtai fibre Co. Ltd. (CN201018898) (2012). Plant stem leaf fibre in device for extracting extraction device for fibre in plant stems and leaves.
[21] Nguyen, NK., Nguyen, VT. (2023). A Prototype of Lotus Fiber Extracting Machine. In: Nguyen, D.C., Vu, N.P., Long, B.T., Puta, H., Sattler, KU. (eds) Advances in Engineering Research and Application. ICERA 2022. Lecture Notes in Networks and Systems, vol 602. Springer, Cham.
[22] Tran Thanh Tung, Nguyen Van Tinh, Dinh Thi Phuong Thao, Tran Vu Minh (2023). Development of a prototype 6 degree of freedom robot arm. Results in Engineering. Volume 18, June 2023, 101049.
[23] Tung, P. D., Watanabe, T., & Nagata, K. (2023). Large-Eddy Simulation of a Flow Generated by a Piston-driven Synthetic Jet Actuator. CFD Letters, 15(8), 1–18.
[24] Pham Duy, T., Watanabe, T., & Nagata, K. (2023). LES Investigation of a Piston-driven Synthetic Jet Actuator with Multiple Orifices. CFD Letters, 16(1), 150–170.
[25] Skiba, K (2019). Designing and FEM simulation of the helicopter rotor and hub. IOP Conference Series: Materials Science and Engineering, 710 012003.
[26] Kasim, A.N., Selamat, M.Z., Aznan N., Sahadan S.N., Daud M.A.M., Salleh S., Jumaidin R. (2019). Effect of pineapple leaf fibre loading on the properties of pineapple leaf fibre – polypropylene composite. Computers and Electronics in Agriculture, Vol. 158, pp. 335-344.